



# Geochronology of sediment cores from the Vefsnfjord, Norway

H.E. Heldal<sup>a,\*</sup>, L. Helvik<sup>a</sup>, P. Appleby<sup>b</sup>, H. Haanes<sup>c</sup>, A. Volynkin<sup>a</sup>, H. Jensen<sup>d</sup>, A. Lepland<sup>d</sup>

<sup>a</sup> Institute of Marine Research, P.O. Box 1870, Nordnes, NO-5817, Bergen, Norway

<sup>b</sup> University of Liverpool, Liverpool L69 3BX, United Kingdom

<sup>c</sup> Norwegian Radiation and Nuclear Safety Authority, P.O. Box 329, Skøyen, NO-0213, Oslo, Norway

<sup>d</sup> Geological Survey of Norway, P.O. Box 6315, Torgarden, NO-7491, Trondheim, Norway

## ARTICLE INFO

### Keywords:

Vefsnfjord

Norway

Sediment supply rates

<sup>210</sup>Pb-dating

<sup>137</sup>Cs

Radioactive contamination

## ABSTRACT

The sedimentary environment is a repository and carrier for a variety of pollutants, and sediment transport from land to coastal areas is an important environmental process. In the present study, we use <sup>210</sup>Pb/<sup>226</sup>Ra and <sup>137</sup>Cs in sediment cores to assess sediment supply rates at four sites within the Vefsnfjord in Nordland county, Norway. This area was highly affected by fallout from the Chernobyl accident in 1986 and inventories of <sup>137</sup>Cs in the fjord are much higher than in many other Norwegian fjords. Sedimentation rates between 0.042 and 0.25 g cm<sup>-2</sup> y<sup>-1</sup> (0.060 and 0.38 cm y<sup>-1</sup>) were determined using a combination of the Constant Rate of Supply (CRS) and Constant Flux:Constant Sedimentation rate (CF:CS) models. Well-defined <sup>137</sup>Cs concentration peaks were used as a supplementary tool to the <sup>210</sup>Pb dating methods.

## 1. Introduction

Use of the naturally occurring radionuclide lead-210 (<sup>210</sup>Pb) (half-life 22.30 ± 0.22 years (Schöttzig and Schrader, 1993)) has in recent decades become the most common method for determining the age of sediments deposited during the past 100 years or so. The origin and distribution of <sup>210</sup>Pb in the environment are described in e.g. the classic papers by Goldberg (1963), Koide et al. (1972) and Turekian et al. (1977). Briefly, disequilibrium between <sup>210</sup>Pb and its long-lived precursor radium-226 (<sup>226</sup>Ra) (half-life 1600 ± 7 years (Bé et al., 2013)) arises through diffusion of the intermediate gaseous isotope radon-222 (<sup>222</sup>Rn) (half-life 3.8232 ± 0.0008 days (Bé et al., 2013)). A fraction of the <sup>222</sup>Rn atoms produced by the decay of <sup>226</sup>Ra in soils escape into the atmosphere where they decay through a series of short-lived radionuclides to <sup>210</sup>Pb. This <sup>210</sup>Pb is removed from the atmosphere by rain, snow or dry deposition, falling either onto the land surface where it is retained in surface soils (Benninger et al., 1975), or into lakes, fjords or oceans. <sup>210</sup>Pb falling directly into the sea is scavenged from the water column by organic matter and mineral particles and incorporated in sediments accumulating on the seabed. In near-shore waters the sediments may also include a fraction of <sup>210</sup>Pb initially deposited on land surfaces and transported with runoff to the fjord.

The <sup>210</sup>Pb in marine (including fjord) sediments thus has two components: *supported* and *unsupported* <sup>210</sup>Pb. Supported <sup>210</sup>Pb derives from

the in situ decay of <sup>226</sup>Ra contained within the sediments. Because of the low diffusivity of <sup>222</sup>Rn in saturated sediments, losses from the sediment column are negligible and supported <sup>210</sup>Pb can in most situations be assumed equal to (in secular equilibrium with) <sup>226</sup>Ra at all core depths. Unsupported <sup>210</sup>Pb is the fraction deriving from atmospheric fallout. In practice, it is measured by the extent to which total <sup>210</sup>Pb activity concentrations exceeds <sup>226</sup>Ra activity concentrations. Unsupported <sup>210</sup>Pb in the sediment column reduces over time according to the simple exponential radioactive decay law. The extent of the decline, if known, can be used to determine the sediment age.

The anthropogenic radionuclide cesium-137 (<sup>137</sup>Cs) (half-life 30.05 ± 0.08 years (Bé et al., 2013)) has been detected in all parts of the earth's surface, from the Arctic to the Antarctic. The most widespread source is fallout from atmospheric testing of nuclear weapons. Such tests started in the early 1950s, reached a peak in the early 1960s and declined to negligible levels during the 1970s following implementation of the 1963 treaty banning atmospheric tests. Although there has been some <sup>137</sup>Cs contamination along the Norwegian coast due to discharges from the UK Sellafield nuclear plant in the mid-to-late 1970s, the main source since then has been from the 1986 Chernobyl reactor fire. Although fallout from that event occurred in many parts of north-west Europe, including Norway (Backe et al., 1986), its distribution was very uneven and dependent on the amount of rainfall when the radioactive cloud was overhead. Records from Norwegian surface soils show that parts of

\* Corresponding author.

E-mail address: [hilde.elise.heldal@hi.no](mailto:hilde.elise.heldal@hi.no) (H.E. Heldal).

<https://doi.org/10.1016/j.marpolbul.2021.112683>

Received 4 March 2021; Received in revised form 25 June 2021; Accepted 27 June 2021

Available online 2 July 2021

0025-326X/© 2021 The Authors. Published by Elsevier Ltd. This is an open access article under the CC BY license (<http://creativecommons.org/licenses/by/4.0/>).

central Norway (Oppland, Hedmark, Trøndelag and Nordland counties, Fig. 1) were highly affected. In some areas, the amounts of  $^{137}\text{Cs}$  deposited in just a few days were orders of magnitude higher than the bomb test residuals. In the area of Nordland surrounding Vefsnfjord, fallout was more than  $20,000 \text{ Bq m}^{-2}$  (Backe et al., 1987). Sources of contamination within the fjord will include both direct fallout and runoff from the adjacent land surfaces.

Results from Norway's national monitoring programme Radioactivity in the Marine Environment (RAME; [www.dsa.no](http://www.dsa.no)) show that surface sediments (0–2 cm) in Vefsnfjord during the period 2002–2018 had  $^{137}\text{Cs}$  concentrations two orders of magnitude higher than in open Norwegian sea areas (NRPA, 2004, 2011, 2012; Skjerdal et al., 2015, 2017, 2020). Since sediments deposited around the time of Chernobyl fallout had even higher levels of  $^{137}\text{Cs}$  contamination, the  $^{137}\text{Cs}$  peaks in sediment profiles can reasonably be interpreted as dating from 1986. Determining the depth of the  $^{137}\text{Cs}$  peak can thus be used as a supplementary age constraining tool to the  $^{210}\text{Pb}$  dating method.

Knowledge and understanding of the supply of sediments to Vefsnfjord is important to comprehend the environmental impact of regional pollution, including the fallout after a nuclear accident. The results from the present study can also be used to draw parallels to other fjord systems. The present study uses  $^{210}\text{Pb}$  and  $^{137}\text{Cs}$  in sediment cores

to assess sediment supply rates at four locations within Vefsnfjord. It forms part of a larger project, which also includes mapping the distribution of natural and anthropogenic radionuclides in Vefsnfjord, grain-size analyses, and total sulphur, total carbon and total organic carbon contents (Heldal et al., in prep). A description of the bathymetry and hydrography of Vefsnfjord is given in Heldal et al. (in prep).

## 2. Materials and methods

### 2.1. Sample collection and preparation

Sediment cores were collected onboard R/V “Kristine Bonnevie” 28.10.2018 using a “Smøgen” box corer (area of  $30 \text{ cm} \times 30 \text{ cm}$  and depth of 40 cm) at four sites in the Vefsnfjord (Fig. 1, Table 1). Three parallel sediment cores were collected from a single box corer at each site. One core was collected to study the vertical distribution of grain-size, total sulphur (TS) and total organic carbon (TOC) whereas two cores were collected to study the vertical distribution of a range of radionuclides (the natural radionuclides potassium-40 ( $^{40}\text{K}$ ),  $^{226}\text{Ra}$ , radium-228 ( $^{228}\text{Ra}$ ),  $^{210}\text{Pb}$  and the anthropogenic radionuclide  $^{137}\text{Cs}$ ). The  $^{137}\text{Cs}$  and  $^{210}\text{Pb}/^{226}\text{Ra}$  data were used to determine the geochronology at each site, which is reported in the present paper. The results

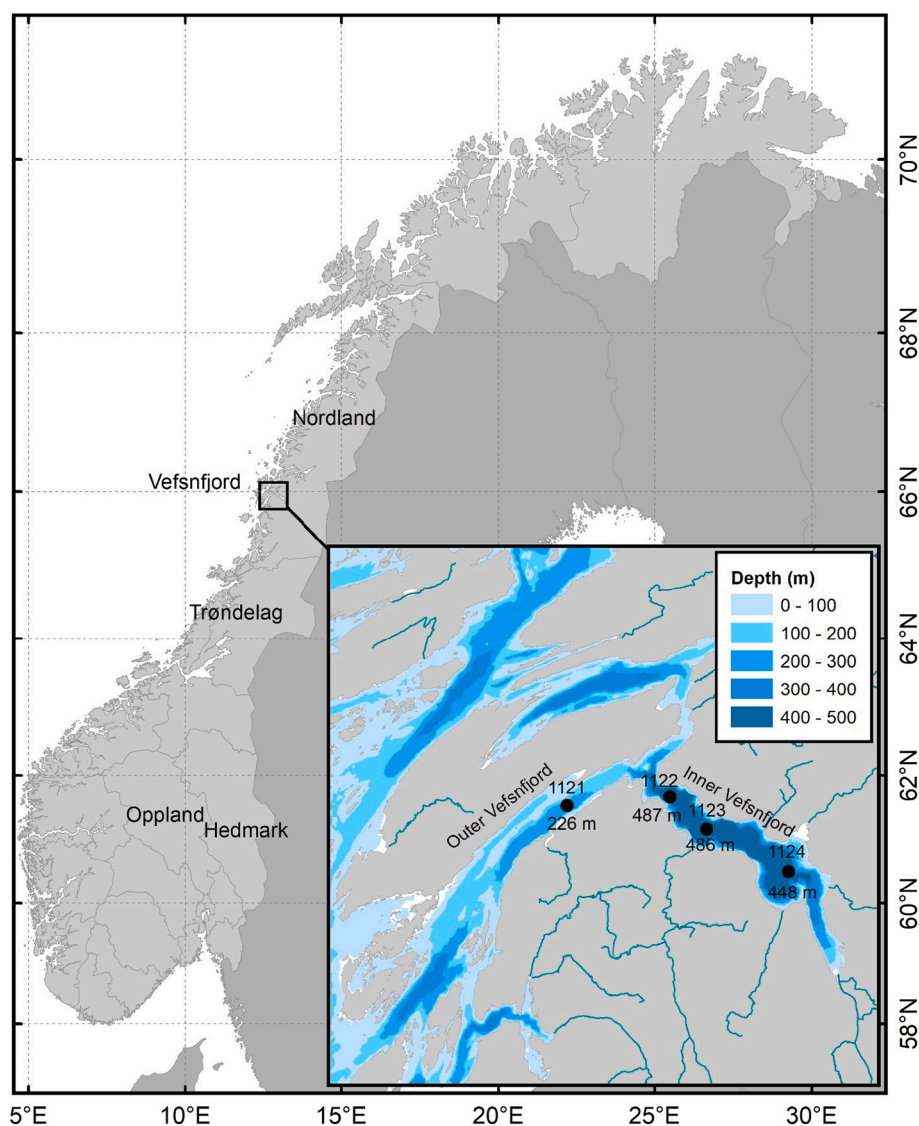


Fig. 1. Map of Norway showing Oppland, Hedmark, Trøndelag and Nordland counties and location of the Vefsnfjord. Inset: Bathymetry of the Vefsnfjord, positions of the four sampling sites and their echo depths (m). Major rivers draining into the fjord are shown.

**Table 1**  
Sediment cores collected for geochronology studies in the Vefsnfjord.

Sample ID	Latitude			Longitude			Echo depth (m)	Length of core (cm)	Number of samples
1121-1	65	57.39	N	12	44.90	E	226	20	15
1121-2	65	57.39	N	12	44.90	E	226	19	15
1122-1	65	57.72	N	12	54.77	E	487	14	12
1122-2	65	57.72	N	12	54.77	E	487	14	12
1123-1	65	56.46	N	12	58.31	E	486	18	14
1123-2	65	56.46	N	12	58.31	E	486	16	13
1124-1	65	54.79	N	13	6.15	E	448	12	11
1124-2	65	54.79	N	13	6.15	E	448	13	12

from analyses of grain-size, TS, TOC and radionuclides are reported in [Heldal et al. \(in prep\)](#).

The sediment cores were collected by pushing PVC tubes of 40 cm length and 10 cm inner diameter into the box core. The bottom ends of the PVC tubes were sharpened to minimize disturbance and the effect of sediment compaction. The cores were cut into 1 cm slices (0–10 cm) and 2 cm slices from 10 cm to the bottom of the core onboard the ship. The samples were transferred to pre-weighed aluminum containers, and their wet weights determined. They were then stored frozen at  $-20^{\circ}\text{C}$  until further preparation took place at Institute of Marine Research (IMR). At the laboratory, the samples were freeze-dried using a CHRIST ALPHA 1–4 freeze dryer and their dry weights (d.w.) determined once a constant weight was achieved. The samples were thereafter homogenized using a Retsch Planetary Ball Mill PM 100.

## 2.2. Analyses of $^{137}\text{Cs}$ , $^{210}\text{Pb}$ and $^{226}\text{Ra}$ by gamma spectrometry

Homogenized samples were transferred to 60 ml polypropylene (PP) counting geometries. Sample weights varied from 43.6 to 70.7 g d.w. The samples were vacuum sealed in an aluminum-lined BoPET bag using a Turbovac T20 Table Top Vacuum Packing Machine to prevent loss of  $^{222}\text{Rn}$ . The samples were thereafter stored for at least four weeks prior to gamma analysis to establish a secular equilibrium between  $^{226}\text{Ra}$  and its progeny ([Gäfvert and Mauring, 2013](#)).

The analytical method for measuring  $^{137}\text{Cs}$  is accredited in accordance with the standard ISO 17025. The calibration and validation sources are traceable to national standards (NPL B180222, VNIIM 252/2000). The methods for determining  $^{210}\text{Pb}$  and  $^{226}\text{Ra}$  are not accredited but are calibrated using sources traceable to national standards (PTB SRM numbers RARB15075 and RBRB15076) and other reference materials (IAEA-RGU-1). The calibration and validation sources had the same geometry and similar density as the samples. The methods are regularly verified by participation in national and international inter-comparison exercises.

The radionuclide content was determined using two low-background ORTEC High Purity Germanium (HPGe) detector systems: one N-type coaxial HPGe-detector (model no. GMX-M5970P-S) with preamplifier (model no. 257N) equipped with X-Cooler electric cryostat cooling system and DSPEC multichannel analyser; and one P-type coaxial HPGe-detector (model no. GEM-S8530P4-RB) with preamplifier (model no. A257P) equipped with X-Cooler III electric cryostat cooling system and DSPEC-50 multichannel analyser. Relative efficiencies of the detectors at 1.33 MeV were 47% and 52%, respectively. Analytical uncertainties are due to uncertainty in sample preparation, calibration standards, calibration methods, counting statistics and background correction, and are in the results given as  $\pm 2\sigma$ . Counting times varied from approximately 65,000 to 270,000 s.

The  $^{137}\text{Cs}$  content was determined using the 661.7 keV gamma peak. No  $^{137}\text{Cs}$  in background was detected. The  $^{210}\text{Pb}$  content was determined according to the method described by [Sværen \(2010\)](#). The method includes corrections for self-absorption of the 46.5 keV gamma peak of  $^{210}\text{Pb}$ . Corrections were carried out using a 255 kBq  $^{210}\text{Pb}$  point source (QSA Global GmbH). The  $^{226}\text{Ra}$  content was determined using gamma peaks of the decay products  $^{214}\text{Pb}$  (295.2 keV and 351.9 keV) and  $^{214}\text{Bi}$

(609.3 keV). Variation in the radon and thoron background levels was controlled by routine background measurements. Background peaks were accounted for by Peak Background Correction (PBC) in the Gamma Vision® software. Radionuclide results for the pair of cores from each site were combined to form a single record. Uncertainties in the combined quantities were calculated using the calculus of propagation of errors.

## 2.3. Determination of age of the sediment layers and sedimentation rates

Sediment ages were initially calculated using the Constant Rate of Supply (CRS) model as described by [Appleby and Oldfield \(1978, 1983\)](#). This assumes that the constant atmospheric flux is reflected in a constant rate of supply of  $^{210}\text{Pb}$  to the sediment record. Non-monotonic down-core variations in  $^{210}\text{Pb}$  in a number of the Vefsnfjord cores precluded use of the alternative Constant Initial Concentration (CIC) model ([Appleby and Oldfield, 1978](#)). Although there is no a priori reason to suppose that either of these simple models is applicable in the marine environment, the CRS model provides a useful first estimate. Discrepancies between the  $^{210}\text{Pb}$  results and the independent 1986 date determined from the  $^{137}\text{Cs}$  record may be caused by small but significant changes to the  $^{210}\text{Pb}$  supply rate. Corrections to the raw  $^{210}\text{Pb}$  dates can then be made by applying the CRS model in a piecewise way using the  $^{137}\text{Cs}$  date as a reference point ([Appleby, 2001](#)). Where the core does not reach  $^{210}\text{Pb}/^{226}\text{Ra}$  equilibrium the CRS model calculations always include an estimate of any missing unsupported  $^{210}\text{Pb}$  below the base of the core. The methods used for doing this are explained in [Appleby \(2001\)](#). Where the core falls well short of the equilibrium depth, the mean  $^{210}\text{Pb}$  flux can be calculated directly using chronostratigraphic dates (1986 or 1963) as reference points. This too is detailed in [Appleby \(2001\)](#).

Where the unsupported  $^{210}\text{Pb}$  activity declines exponentially with depth, mean accumulation rates can be calculated using the least squares fit procedure exemplified in [Goldberg \(1963\)](#). Sometimes referred to as the Constant flux:Constant sedimentation rate (CF:CS) model, this too can be applied either in a piecewise way or to the record as a whole.

The  $^{210}\text{Pb}$  calculations all use the cumulative dry mass ( $\text{g cm}^{-2}$ ) as the depth parameter. Unlike the volumetric rate ( $\text{cm y}^{-1}$ ), the dry mass value ( $\text{g cm}^{-2} \text{y}^{-1}$ ) is unaffected by sediment compaction either before or during coring.

Uncertainties in the sediment ages and sedimentation results were determined from the analytical uncertainties using the calculus of propagation of errors. [Binford \(1990\)](#) estimates that with 95% confidence these typically range from about 1–2 (10–20%) years at ten years of age, 10 to 20 (10–20%) years at 100 years of age and 8–90 (5–60%) years at 150 years age.

## 3. Results

### 3.1. Radiometric measurements

Although there were small differences between the individual records, for the most part these can be attributed to statistical

uncertainties in the radiometric assays, and small variations in the sampling and sample preparation procedures.

Table 2 summarises a number of key parameters from each site including the mean  $^{226}\text{Ra}$  (supported  $^{210}\text{Pb}$ ) activity concentration ( $\text{Bq kg}^{-1}$ ), surficial unsupported  $^{210}\text{Pb}$  activity concentration ( $\text{Bq kg}^{-1}$ ), unsupported  $^{210}\text{Pb}$  inventory ( $\text{Bq m}^{-2}$ ), mean  $^{210}\text{Pb}$  flux (or supply rate,  $\text{Bq m}^{-2} \text{ y}^{-1}$ ), and the  $^{137}\text{Cs}$  inventory ( $\text{Bq m}^{-2}$ ). The  $^{210}\text{Pb}$  flux is calculated using the equation.

$$P = \lambda A(0)$$

where  $\lambda$  is the  $^{210}\text{Pb}$  radioactive decay constant ( $0.03114 \text{ y}^{-1}$ ) and  $A(0)$  the unsupported  $^{210}\text{Pb}$  inventory.

Supported  $^{210}\text{Pb}$  ( $^{226}\text{Ra}$ ) is relatively uniform both temporally (down core) and spatially (across cores) (Fig. 2, Supplementary Material (SM) 1) possibly indicating that sediment sources within Vefsnfjord have remained relatively constant during the past 100 years or so. A small increase in values in the near-surface sediments at sites 1122, 1123 and to a lesser extent 1124, may be due to recent changes.

Unsupported  $^{210}\text{Pb}$  in the surficial sediments range from  $160 \text{ Bq kg}^{-1}$  in the outer fjord to between 185 and  $223 \text{ Bq kg}^{-1}$  in the inner fjord (Table 2). Slightly higher values at site 1123 in the middle of the inner fjord are consistent with a slightly finer grain size of sediments at this site compared to 1122 and 1124 (see Haldal et al., in prep). At all four sites the mean  $^{210}\text{Pb}$  flux is significantly higher than the estimated atmospheric flux ( $\sim 100 \text{ Bq m}^{-2} \text{ y}^{-1}$ ; Peirson et al., 1966). Possible causes include sediment focussing, and erosional inputs from the surrounding catchment areas. The very high  $^{137}\text{Cs}$  inventories ( $16,719\text{--}23,319 \text{ Bq m}^{-2}$ ) show that records of this artificial radionuclide are mainly due to fallout from the 1986 Chernobyl accident.

### 3.2. Radiometric records

Plots of total, supported and unsupported  $^{210}\text{Pb}$  activity concentrations ( $\text{Bq kg}^{-1}$ ) versus depth are shown in Fig. 2, and for  $^{137}\text{Cs}$  ( $\text{Bq kg}^{-1}$ ) in Fig. 3. The numerical values are available in SM 1. At all four sites the  $^{210}\text{Pb}$  record falls short of the point at which total  $^{210}\text{Pb}$  is in equilibrium with the supported  $^{210}\text{Pb}$ . In consequence, the period of time spanned in the studied sediment successions is less than the theoretical maximum of around 5  $^{210}\text{Pb}$  half-lives or  $\sim 110$  years. All cores do however have relatively distinct peaks in the  $^{137}\text{Cs}$  records (Fig. 3) that can be used to identify the depth of sediments deposited in 1986, the time of the Chernobyl accident.

#### 3.2.1. Site 1121

Following an initial steep decline, unsupported  $^{210}\text{Pb}$  has a significant non-monotonic feature between 5 and 12 cm (Fig. 2 a) that presumably records an episode of more rapid sediment accumulation. Below this feature concentrations decline steeply and more or less exponentially with depth. A well-defined  $^{137}\text{Cs}$  peak places 1986 at a depth of between 10 and 14 cm (Fig. 3 a). It follows that the episode of rapid accumulation must have taken place post-1986. Total  $^{210}\text{Pb}$  at the base of the core slightly exceeds that of the supported  $^{210}\text{Pb}$ .

**Table 2**

Key parameters for each site including the mean  $^{226}\text{Ra}$  (supported  $^{210}\text{Pb}$ ) activity concentration, unsupported  $^{210}\text{Pb}$  surficial activity concentration, inventory and flux, and the  $^{137}\text{Cs}$  inventory.

Site	$^{226}\text{Ra}$		Unsupported $^{210}\text{Pb}$				$^{137}\text{Cs}$	
	Mean activity conc.		Surficial activity conc.		Inventory		Inventory	
	$\text{Bq kg}^{-1}$	$\pm$	$\text{Bq kg}^{-1}$	$\pm$	$\text{Bq m}^{-2}$	$\text{Bq m}^{-2} \text{ y}^{-1}$	$\text{Bq m}^{-2}$	$\pm\%$
1121	26	2	160	8	8400	262	23,319	2.7
1122	33	4	189	9	9259	288	17,928	2.6
1123	32	3	223	11	9169	286	16,719	2.3
1124	28	3	185	9	10,433	325	18,010	2.4

#### 3.2.2. Site 1122

The  $^{210}\text{Pb}$  record at this site also falls short of the  $^{210}\text{Pb}/^{226}\text{Ra}$  equilibrium depth (Fig. 2 b). Extrapolation of the data indicates that this would be reached at a depth of around 20 cm. Activity concentrations in the deepest samples analysed (12–14 cm) suggest that the cores span around 4  $^{210}\text{Pb}$  half-lives ( $\sim 90$  years). Unsupported  $^{210}\text{Pb}$  decline more or less exponentially with depth, apart possibly from a small reduction in the gradient in the uppermost 2 cm. It follows that sedimentation rates at this site have been relatively constant throughout much of the recent past.

$^{137}\text{Cs}$  concentrations have a well-defined peak in the 6–7 cm sample (Fig. 3 b) that presumably records fallout from the 1986 Chernobyl accident.

#### 3.2.3. Site 1123

The  $^{210}\text{Pb}$  record is similar to site 1122 apart from an intermediate section between 6 and 9 cm in which concentrations are virtually constant (Fig. 2 c). This feature may record an episode of more rapid sediment accumulation. Excluding this episode, sedimentation rates appear to have been relatively constant.

$^{137}\text{Cs}$  concentrations have a relatively well-defined peak between 7 and 8 cm (Fig. 3 c) recording the 1986 Chernobyl fallout event.

#### 3.2.4. Site 1124

The base of the total  $^{210}\text{Pb}$  record is significantly above the  $^{210}\text{Pb}/^{226}\text{Ra}$  equilibrium depth (Fig. 2 d). Concentrations in the deepest sample suggest that the cores span less than three  $^{210}\text{Pb}$  half-lives ( $<66$  years). Since unsupported  $^{210}\text{Pb}$  decline more or less exponentially with depth, it follows that sedimentation rates at this site have been relatively constant.

A well-defined  $^{137}\text{Cs}$  peak places 1986 within the 6–7 cm sample (Fig. 3 d).

### 3.3. Core chronologies

Results of the  $^{210}\text{Pb}$  age versus depth calculations, and sedimentation rate determinations are shown in Figs. 4–7. The numerical values are available in SM 2. Table 3 summarises mean sedimentation rates at each site before and after 1986.

#### 3.3.1. Site 1121

Because of the significant non-monotonic variation in unsupported  $^{210}\text{Pb}$  activity between 5 and 12 cm (Fig. 2 a) it was only possible to date sediments from this site using the CRS model. The raw calculations suggested a relatively low sedimentation rate during much of the 20th century followed by an episode of much more rapid accumulation towards the end of the century. There was however a significant discrepancy between the  $^{210}\text{Pb}$  and  $^{137}\text{Cs}$  results. The  $^{210}\text{Pb}$  calculations placed 1986 within the 8–9 cm sample, significantly above the 1986 depth indicated by a well-defined  $^{137}\text{Cs}$  peak (10–14 cm, Fig. 3 a). The cause of the discrepancy appears to be a significant increase in the  $^{210}\text{Pb}$  supply rate associated with the late 20th century episode of rapid sedimentation. The discrepancy can be resolved by applying the CRS model in a piecewise way to the pre-1986 and post-1986 records



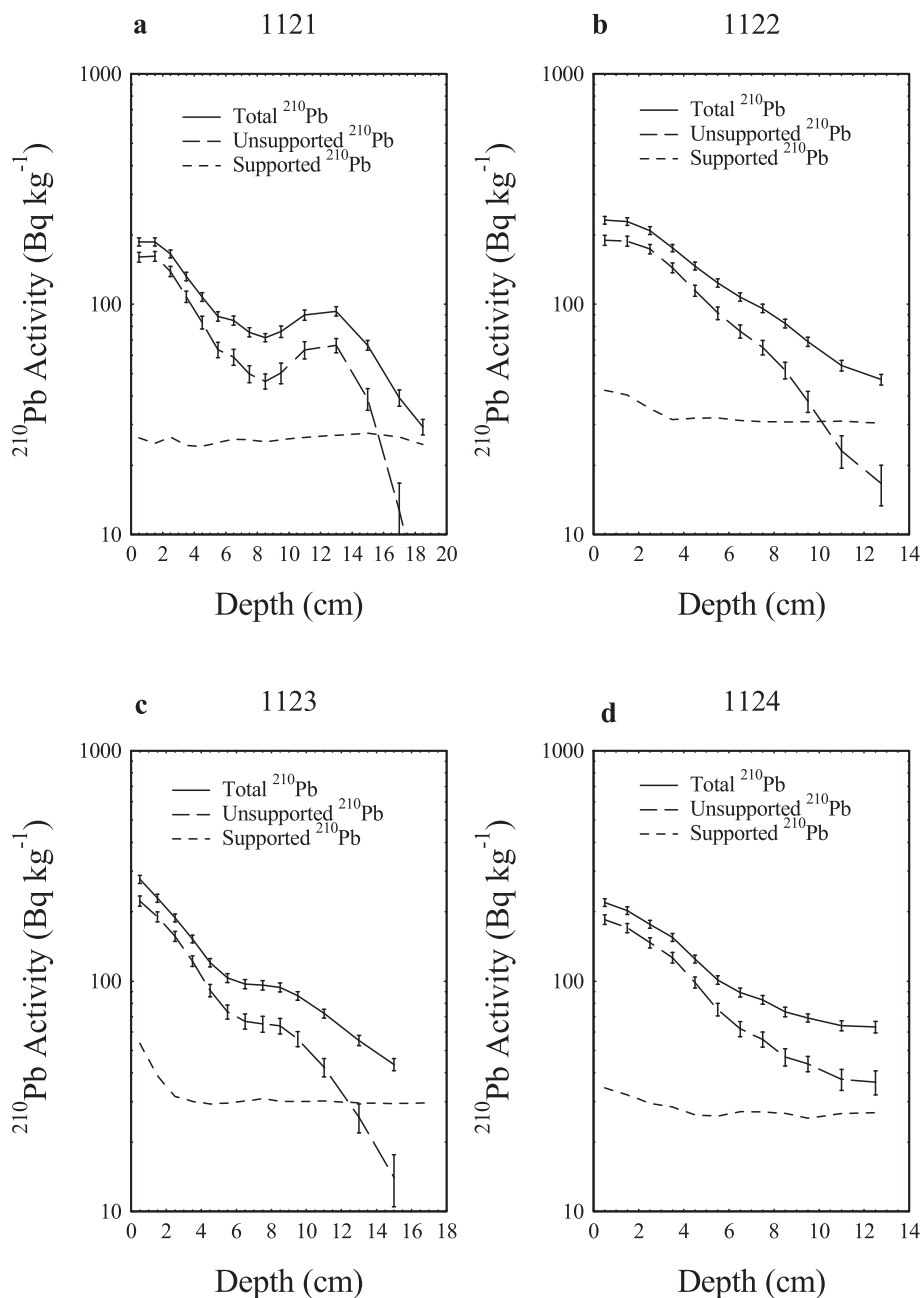


Fig. 2. a-d. Vertical distribution ( $\text{Bq kg}^{-1}$  d.w.) of total  $^{210}\text{Pb}$ , supported  $^{210}\text{Pb}$  and unsupported  $^{210}\text{Pb}$  in cores from the four sites.

(Appleby, 2001). The results of the revised calculations (shown in Fig. 4) suggest that up until the 1980s sedimentation rates had been relatively uniform, with a mean value  $0.042 \pm 0.005 \text{ g cm}^{-2} \text{ y}^{-1}$  ( $0.060 \pm 0.008 \text{ cm y}^{-1}$ ). The period of rapid accumulation appears to have persisted from the mid-1980s through to around 2010, since when sedimentation rates have been relatively uniform though at a higher value than before. The mean post-1986 sedimentation rate is calculated to be  $0.25 \pm 0.03 \text{ g cm}^{-2} \text{ y}^{-1}$  ( $0.38 \pm 0.04 \text{ cm y}^{-1}$ ).

### 3.3.2. Site 1122

The  $^{210}\text{Pb}$  dates for the cores collected at this site are relatively unequivocal. Further, since unsupported  $^{210}\text{Pb}$  declines more or less exponentially with depth (Fig. 2 b), all models indicate relatively uniform sedimentation. The mean value for the entire period (pre- and post-1986) is calculated to be  $0.12 \pm 0.01 \text{ g cm}^{-2} \text{ y}^{-1}$  ( $0.14 \pm 0.02 \text{ cm y}^{-1}$ ). Ages calculated using this value (Fig. 5) place 1986 within the 5–6 cm

sample. There is thus a small discrepancy with the  $^{137}\text{Cs}$  results, which suggest placing 1986 in the 6–7 cm sample (Fig. 3 b). Given the unequivocal nature of the  $^{210}\text{Pb}$  results, the most likely cause of the discrepancy is smearing of the initial signal coupled with a degree post-depositional migration. Although the fallout event lasted no more than a few days, high  $^{137}\text{Cs}$  concentrations are recorded in 3 slices, from 5 to 8 cm, spanning 21 years.

### 3.3.3. Site 1123

Calculations using the CRS model support the suggestion that the section between 6 and 9 cm in which concentrations are virtually constant (Fig. 2 c) does record an episode of more rapid sediment accumulation. Its location close to the peak in  $^{137}\text{Cs}$  concentrations (at 7–9 cm, Fig. 3 c) dates this event to around the same time as the 1986 Chernobyl accident. Since the raw  $^{210}\text{Pb}$  ages place 1986 above the  $^{137}\text{Cs}$  peak, in the 6–7 cm sample, it is likely that increased sedimentation

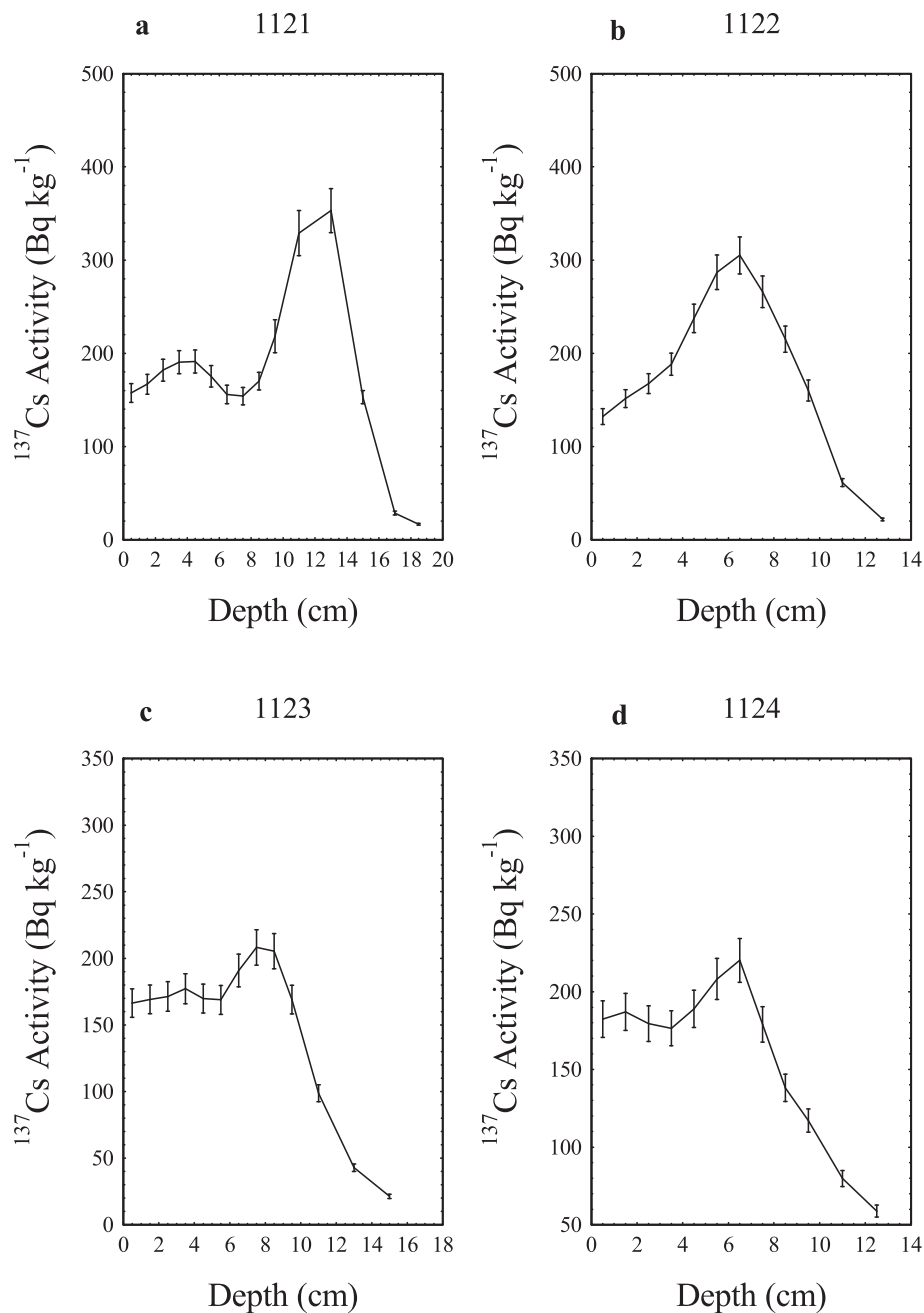


Fig. 3. a-d. Vertical distribution ( $\text{Bq kg}^{-1} \text{ d.w.}$ ) of  $^{137}\text{Cs}$  in sediment cores from the four sites.

rates were associated with an increase in the  $^{210}\text{Pb}$  supply rate. Applying the CRS model in a piecewise way to the pre-1986 and post-1986 records using the  $^{137}\text{Cs}$  peak as a reference level (Appleby, 2001), the revised calculations suggest that up until the early 1980s sedimentation rates were relatively uniform with mean value of  $0.11 \pm 0.02 \text{ g cm}^{-2} \text{ y}^{-1}$  ( $0.12 \pm 0.03 \text{ cm y}^{-1}$ ) (Fig. 6), similar to that at site 1122. The period of more rapid accumulation may have persisted from the mid-1980s through to around the year 2000. Since then sedimentation rates have again been relatively uniform with a mean value of  $0.18 \pm 0.03 \text{ g cm}^{-2} \text{ y}^{-1}$  ( $0.25 \pm 0.04 \text{ cm y}^{-1}$ ), a little higher than the pre-1980 value (Fig. 6).

### 3.3.4. Site 1124

Because of the brevity of the  $^{210}\text{Pb}$  record it was not possible to date this core using the CRS model. Since unsupported  $^{210}\text{Pb}$  declines more or less exponentially with depth (Fig. 2 d), it is however likely that sedimentation rates have been relatively constant, and the mean

sedimentation rate for the entire period (pre- and post-1986) can therefore be calculated using the CF:CS model. The results of these calculations suggest a value of  $0.18 \pm 0.03 \text{ g cm}^{-2} \text{ y}^{-1}$  ( $0.19 \pm 0.03 \text{ cm y}^{-1}$ ), significantly higher than the pre-1980 sedimentation rates at 1122 and 1123 (Fig. 7). Ages calculated using this value place 1986 within the 6–7 cm sample, in good agreement with the 1986 depth suggested by the  $^{137}\text{Cs}$  record (Fig. 3 d).

## 4. Discussion

Conditions at the different sites are affected by a number of factors including grain size, content of organic matter, sediment supply rates, and the  $^{210}\text{Pb}$  flux. The highest sediment supply rates are found post-1986 at site 1121 in the outer Vefsnfjord (Table 3). This is also the site with the lowest surficial activity concentrations of  $^{210}\text{Pb}$ , the lowest  $^{210}\text{Pb}$  inventory and the highest  $^{137}\text{Cs}$  inventory (Table 2). This part of

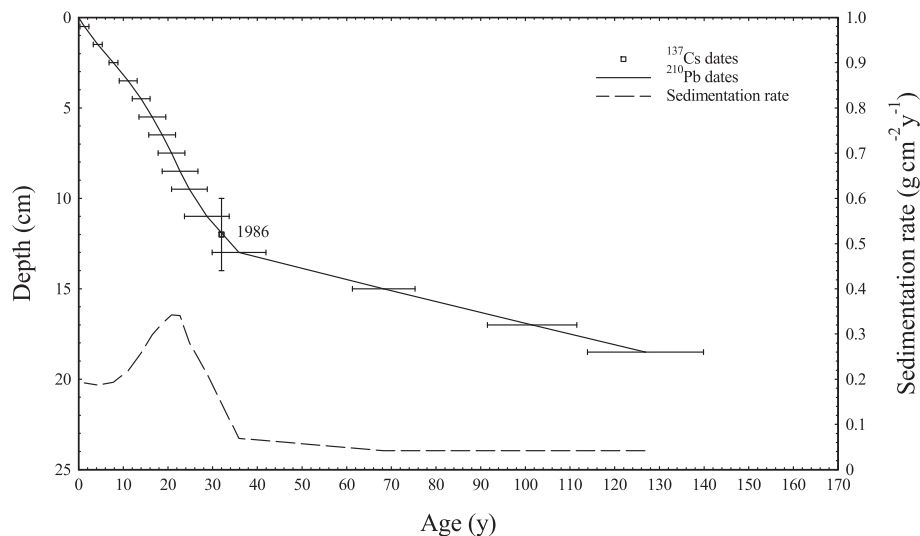


**Fig. 4.** Radiometric chronology at site 1121 showing the 1986 depth suggested by the  $^{137}\text{Cs}$  record and the  $^{210}\text{Pb}$  dates and sedimentation rates calculated using the piecewise CRS model with 1986  $^{137}\text{Cs}$  date as a reference point.

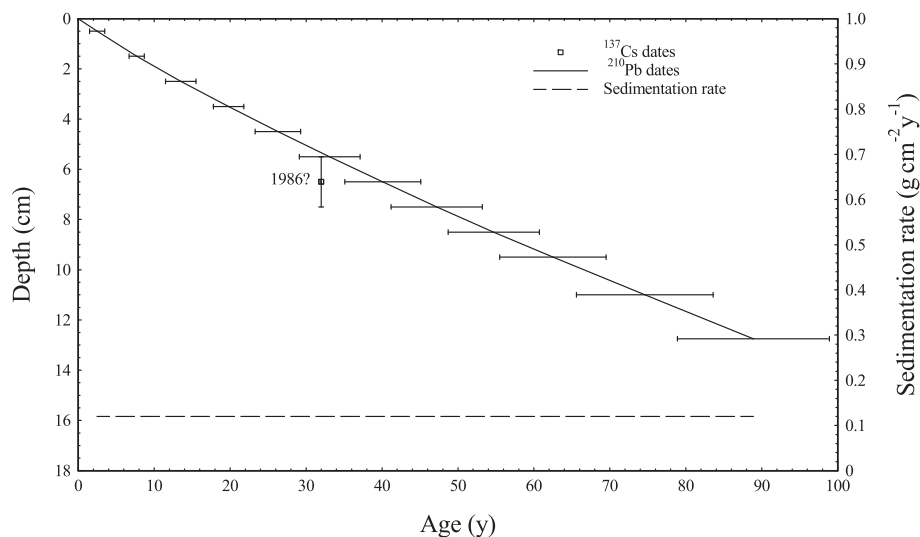


**Fig. 5.** Radiometric chronology at site 1122 showing the  $^{210}\text{Pb}$  dates and sedimentation rate calculated using the mean sedimentation rate determined by the CF:CS model and the 1986 depth suggested by the  $^{137}\text{Cs}$  record. There is no obvious reason for the discrepancy between the two dating methods.

the fjord has steep fjord sides with 1 km high peaks and no major river outlets that can supply sediments. Thus, the catchment area is small with potentially low supply of  $^{210}\text{Pb}$ , but high relief facilitating higher local erosion and sediment supply rates. If bathymetry and/or stratification provide a higher phytoplankton growth in the outer fjord, scavenging of  $^{137}\text{Cs}$  in the water column could be a cause for higher  $^{137}\text{Cs}$  inventory and lower surficial  $^{210}\text{Pb}$  levels at this site. However, this needs to be further investigated.

Slightly higher surficial levels of  $^{137}\text{Cs}$  were observed at the innermost site (1124) (Fig. 3, SM 1). Although levels may be affected by many factors, catchment runoff may be a likely candidate. This part of the fjord is supplied with runoff carrying suspended sediments from the rivers Vefsna, Fusta, Drevjo and Hundåla (see Heldal et al., in prep). Compared to Chernobyl, other sources for  $^{137}\text{Cs}$  in the Vefsnfjord are minor (see e.g. Skjerdal et al., 2020), and should not affect the differences we see between the outer and inner fjord. The large catchment area in the inner fjord may also explain higher levels of  $^{210}\text{Pb}$ , particularly in the middle of the fjord, where finest sediments accumulate.

The depth profiles of  $^{137}\text{Cs}$  have similar trends at all the sampling

sites. However, the cores from the different sites vary both with regards to maximum activity concentrations, and how deep in the sediment column this maximum is found. The cores sampled at site 1121 stand out with both highest maximum activity concentrations of  $^{137}\text{Cs}$ , and the deepest position of the maximum in the core. The latter is due to a higher post-1986 sedimentation rate at this site.

The echo depth at site 1121 is 226 m, while the echo depths at the other three sites inward in the fjord vary from 448 to 487 m, hence bathymetric variations may contribute to the observed differences. Further, the freshwater supply from several rivers affects the salinity of the waters, particularly in the inner part of the fjord (e.g. Haugen et al., 1981; Molvær, 2010). Although most of the fresh water will float on top of the heavier salty water, some may mix downwards and affect the radionuclide distribution in the fjord. Poorer water exchange in the inner part of the fjord, compared to the outer part, may also contribute to the observed differences between the sites.

Sedimentation rates found in this study are similar to those found by Haugen et al. (1981) in cores collected in 1978 at two sites in the inner part of Vefsnfjord (average rates of 0.20 and 0.17  $\text{cm y}^{-1}$ ). They found

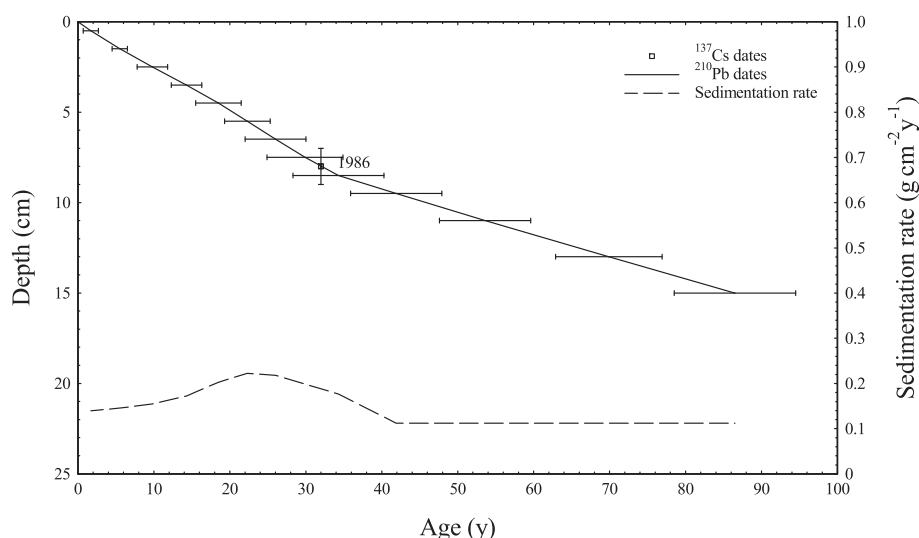


Fig. 6. Radiometric chronology at site 1123 showing the 1986 depth suggested by the  $^{137}\text{Cs}$  record and the  $^{210}\text{Pb}$  dates and sedimentation rates calculated using piecewise CRS model with the 1986  $^{137}\text{Cs}$  date as a reference point.

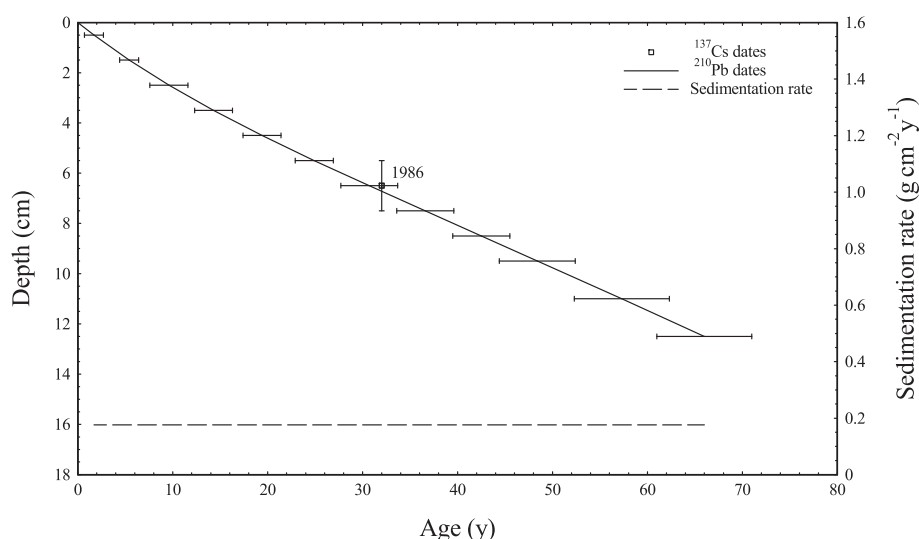


Fig. 7. Radiometric chronology at site 1124 showing the  $^{210}\text{Pb}$  dates and sedimentation rate calculated using the mean sedimentation rate determined by the CF:CS model and the 1986 depth suggested by the  $^{137}\text{Cs}$  record.

Table 3

Mean pre- and post-1986 sedimentation rates ( $\text{g cm}^{-2} \text{y}^{-1}$  and  $\text{cm y}^{-1}$ ). Higher post-1986 volumetric rates at 1122 and 1124 reflect changes in the dry bulk density of sediments towards the top of the core.

Site	Sedimentation rates			
	Pre-1986		Post-1986	
	$\text{g cm}^{-2} \text{y}^{-1}$	$\text{cm y}^{-1}$	$\text{g cm}^{-2} \text{y}^{-1}$	$\text{cm y}^{-1}$
1121	$0.042 \pm 0.005$	$0.060 \pm 0.008$	$0.25 \pm 0.03$	$0.38 \pm 0.04$
1122	$0.12 \pm 0.01$	$0.13 \pm 0.02$	$0.12 \pm 0.01$	$0.17 \pm 0.02$
1123	$0.11 \pm 0.02$	$0.12 \pm 0.03$	$0.18 \pm 0.03$	$0.25 \pm 0.04$
1124	$0.18 \pm 0.03$	$0.17 \pm 0.03$	$0.18 \pm 0.03$	$0.21 \pm 0.03$

an increase in the sedimentation rate at the innermost part of Vefsnfjord 15–20 years before sampling and suggest that this is related to the establishment of Mosjøen Aluminum plant in 1958. It cannot be ruled out that some of the irregularities we see in our cores are also due to activities in Mosjøen Aluminum plant. There may also be other causes

for variations in sediment supply rates in coastal areas. Periods of heavy rainfall may increase the supply of  $^{210}\text{Pb}$  from catchment runoff (Appleby, 2001; Appleby et al., 2019). Fresh water supply varies throughout the year and may vary from year to year.

There are few studies on sedimentation rates from other Norwegian fjords, but one example is the study by Sternal et al. (2017) in Repparfjord in Troms and Finnmark county. Repparfjord has a history of submarine tailings disposal from copper (Cu) mine activities. Sternal et al. (2017) found sedimentation rates based on  $^{210}\text{Pb}$  ranging from 0.04 to 0.47  $\text{cm y}^{-1}$ . The sedimentation rates were somewhat higher in the inner part of the Repparfjord. The sedimentation rates in the Repparfjord are comparable to the ones in Vefsnfjorden (0.060 to 0.38  $\text{cm y}^{-1}$ ).

Sedimentation rates in open sea areas vary widely. Rates ranging from 0.05 to 0.5  $\text{cm y}^{-1}$  are reported in the literature for the North, Norwegian and Barents Seas (e.g. Heldal et al., 2002; Maiti et al., 2010; Huh et al., 1997; www.mareano.no; Zaborska et al., 2008). Organic matter sedimentation in open sea areas is strongly controlled by physiogeographic parameters including distance to shore, sea-ice coverage



and melting as well as pathways and velocities of ocean currents. Sediments accumulation patterns can be highly variable with highest accumulation rates in sheltered depressions. Banks and other extensive areas, on the other hand, have relatively little sedimentation owing to strong ocean currents (Knies et al., 2006; Knies and Martinez, 2009).

$^{210}\text{Pb}$ -dating is a useful tool but has several methodology-traps arising from the underlying assumptions. These necessarily simplify the complex processes delivering fallout  $^{210}\text{Pb}$  to the sediment record. Bioturbation may cause vertical transport of radionuclides in the sediments and thus disturb the exponential decline in  $^{210}\text{Pb}$  activity concentrations. Bottom trawling may disturb the surface of the seafloor and have the same effect. Finally, cross-contamination during sampling and slicing of the cores is also a possible source of error. Therefore, the use of complementary isotopes to determine sediment accumulation is warranted.  $^{137}\text{Cs}$  was used in the present study, but there may be uncertainties associated with the use of this isotope as well, as it may migrate in the sediment column (e.g. Ligeró et al., 2005). The two thorium-isotopes  $^{234}\text{Th}$  and  $^{228}\text{Th}$  both provide information on mixing. Coupling these data to  $^{210}\text{Pb}$  and furthermore to the sediment profile of e.g. Pu-isotopes could make the interpretation much more reliable than if only using  $^{210}\text{Pb}$  and/or  $^{137}\text{Cs}$ , as we did in the present study.

## 5. Conclusions

Geochronology was studied at four sites in Vefsnfjord, Norway, using the naturally occurring radionuclides  $^{210}\text{Pb}$  and  $^{226}\text{Ra}$ . The  $^{137}\text{Cs}$  peak originating from the 1986 Chernobyl accident was used as a supplementary dating tool. Sedimentation rates were determined successfully using either the CF:CS method or the CRS method in a piecewise way with 1986 as a reference date. Sedimentation rates were in the range of  $0.042$  to  $0.25\text{ g cm}^{-2}\text{ y}^{-1}$  ( $0.060$  to  $0.38\text{ cm y}^{-1}$ ) and varied both spatially and temporally. At some of the sites there were small differences between the two cores taken from the same box corer. This difference is probably for the most part attributed to statistical uncertainties in the radiometric assays, and small variations in the sampling and sample preparation procedures.

Coastal areas are important for Norwegian fisheries and aquaculture industry, and therefore particularly vulnerable and susceptible to pollutants. The knowledge of sediment supply rates to coastal areas is highly relevant to Norwegian nuclear preparedness, as it will contribute to a better understanding of the consequences of a potential future nuclear accident.

Supplementary data to this article can be found online at <https://doi.org/10.1016/j.marpolbul.2021.112683>.

## CRedit authorship contribution statement

Geochronology of sediment cores from the Vefsnfjord, Norway (MPB-D-21-00489).

This work is based on a Master project by Lena Helvik (LH). Hilde Elise Heldal (HEH) was LH's main supervisor and Hallvard Haanes (HH) was co-supervisor.

HEH planned the study with input from Henning Jensen (HJ) and HH.

LH and HEH performed the field work.

LH prepared all samples and analysed them using gamma spectrometry with supervision from Andrey Volynkin (AV). LH interpreted the gamma results.

Peter Appleby (PA) was responsible for calculating sediment ages and accumulation rates and generally interpreting the geochronology results.

HJ and Aivo Lepland (AL) were responsible for analyses of grain size, total sulphur, total carbon, total organic carbon and calculation of carbonate content. These data are presented in MPB-D-21-00488, but results are used in the discussion in the present study. HJ and AL contributed to put the radionuclide and geochronology results in a

geological context.

HEH took the lead in writing the manuscript. PA contributed with text related to geochronology. AV was responsible for writing chapter 2.2. HH contributed to the introduction and discussion. HJ and AL wrote the geology parts of the manuscript.

All authors provided critical feedback on the manuscript as a whole and helped shape the research and analyses.

## Declaration of competing interest

The authors declare that they have no known competing financial interests or personal relationships that could have appeared to influence the work reported in this paper.

## Acknowledgements

Thanks are due to the crew of R/V “Kristine Bonnevie” and Penny Lee Liebig (IMR) for assistance with sample collection and sample preparation and Kjell Bakkeplass (IMR) for creating the map.

## References

- Appleby, P.G., Oldfield, F., 1978. The calculation of lead-210 dates assuming a constant rate of supply of unsupported  $^{210}\text{Pb}$  to the sediment. *Catena* 5 (1), 1–8.
- Appleby, P.G., 2001. Chronostratigraphic techniques in recent sediments. In: Last, W.M., Smol, J.P. (Eds.), *Tracking Environmental Change Using Lake Sediments. Volume 1: Basin Analysis, Coring, and Chronological Techniques*. Kluwer Academic Publishers, Dordrecht, The Netherlands, pp. 171–203.
- Appleby, P.G., Oldfield, F., 1983. The assessment of  $^{210}\text{Pb}$  data from sites with varying sediment accumulation rates. *Hydrobiologia* 103, 29–35.
- Appleby, P.G., Semertzidou, P., Piliposian, G.T., Chiverrell, R.C., Schillereff, D.N., Warburton, J., 2019. The transport and mass balance of fallout radionuclides in Brotherswater, Cumbria (UK). *J. Paleolimnol.* 62 (4), 389–407.
- Backe, S., Bjerke, H., Rudjord, A.L., Ugletveit, F., 1986. Nedfall av cesium i Norge etter Tjernobylyllykken (in Norwegian), vol. 5. Statens Institutt for Strålehygiene, Norway, p. 51, 1986.
- Backe, S., Bjerke, H., Rudjord, A.L., Ugletveit, F., 1987. *Radiat. Prot. Dosim.* 18 (2), 105–107.
- Bé, M.-M., Chisté, V., Dulieu, C., Mougeot, X., Browne, E., Baglin, C., Chechev, V.P., Egorov, A., Kuzmenko, N.K., Sergeev, V.O., Kondev, F.G., Luca, A., Galán, M., Huang, X., Wang, B., Helmer, R.G., Schönfeld, E., Dersch, R., Vanin, V.R., de Castro, R.M., Nichols, A.L., MacMahon, T.D., Pearce, A., Arinc, A. Lee, K.B., Wu, S.C., 2013. Monographie BIPM-5—table of radionuclides, vol. 1-7. ISBN 92-822-2248-5.
- Benninger, L.K., Lewis, D.M., Turekian, K.K., 1975. The use of natural  $^{210}\text{Pb}$  as a heavy metal tracer in the river estuarine system. In: Church, T.M. (Ed.), *Marine Chemistry in the Coastal Environment*. Am. Chem. Soc. Symp. Ser. vol. 18, pp. 202–210.
- Binford, M.W., 1990. Calculation and uncertainty analysis of  $^{210}\text{Pb}$  dates for PIRLA project lake sediment cores. *J. Paleolimnol.* 3, 253–267.
- Gärfvert, T., Mauring, A., 2013. Radon tightness of different sample sealing methods for gamma spectrometric measurements of  $^{226}\text{Ra}$ . *Appl. Radiat. Isot.* 81, 92–95.
- Goldberg, 1963. *Geochronology with lead-210*. In: *Radioactive Dating*. Vienna: International Atomic Energy Agency. Symposium Proceedings, pp. 121–131.
- Haugen, I., Knutzen, J., Kvalvågnes, K., Magnusson, J., Rygg, B., Skei, J., 1981. Vefsnfjorden som resipient for avfall fra Mosjøen Aluminiumsverk. Rapport 1. Undersøkelser 1978–1980. Rapportnummer 0–76149. Norwegian Institute for Water Research (NIVA), Oslo (In Norwegian).
- Heldal, H.E., Varskog, P., Foyen, L., 2002. Distribution of selected anthropogenic radionuclides ( $^{137}\text{Cs}$ ,  $^{238}\text{Pu}$ ,  $^{239,240}\text{Pu}$  and  $^{241}\text{Am}$ ) in marine sediments with emphasis on the Spitsbergen-Bear Island area. *Sci. Total Environ.* 293, 233–245.
- Heldal, H.E., Helvik, L., Haanes, H., Volynkin, A., Jensen, H., Lepland, A., 2021. Distribution of Natural and Anthropogenic Radionuclides in Sediments from the Vefsnfjord, Norway (Submitted to *Marine Pollution Bulletin*, in prep).
- Huh, C.-A., Pisias, N.G., Kelley, J.M., Maiti, T.C., Grantz, A., 1997. Natural radionuclides and plutonium in sediments from the western Arctic Ocean: sedimentation rates and pathways of radionuclides. *Deep-Sea Res.* II 44 (8), 1725–1743.
- Knies, J., Martinez, P., 2009. Organic matter sedimentation in the western Barents Sea region: terrestrial and marine contribution based on isotopic composition and organic nitrogen content. *Nor. J. Geol.* 89, 79–89.
- Knies, J., Jensen, H.K.B., Finne, T.E., Lepland, A., Sæther, O.M., 2006. Sediment Composition and Heavy Metal Distribution in Barents Sea Surface Samples: Results from Institute of Marine Research 2003 and 2004 Cruises. NGU Report 2006.067. ISSN 0800-3416.
- Koide, M., Souter, A., Goldberg, E.D., 1972. Marine geochronology with  $^{210}\text{Pb}$ . *Earth Planet. Sci. Lett.* 14 (3), 442–446.
- Ligeró, R.A., Barrera, M., Casas-Ruiz, M., 2005. Levels of  $^{137}\text{Cs}$  in muddy sediments of the seabed of the bay of Cádiz, Spain. Part I. Vertical and spatial distribution of activities. *J. Environ. Radioact.* 80, 75–86.
- Maiti, K., Carroll, J., Benitez-Nelson, C.R., 2010. Sedimentation and particle dynamics in the seasonal ice zone of the Barents Sea. *J. Mar. Syst.* 79, 185–198.

- Molvær, J., 2010. Vefsnfjorden. Rapport O-29321. Norwegian Institute for Water Research, Oslo.
- NRPA, 2004. Radioactivity in the marine environment 2002. Results from the Norwegian National Monitoring Programme (RAME). StrålevernRapport 2004:10. Norwegian Radiation Protection Authority, Østerås.
- NRPA, 2011. Radioactivity in the Marine Environment 2008 and 2009. Results from the Norwegian Monitoring Programme (RAME). StrålevernRapport 2011. Norwegian Radiation Protection Authority, Østerås, p. 4.
- NRPA, 2012. Radioactivity in the marine environment 2010. Results from the Norwegian Monitoring Programme (RAME). StrålevernRapport 2012. Norwegian Radiation Protection Authority, Østerås, p. 10.
- Peirson, D.H., Cambray, R.S., Spicer, G.S., 1966. Lead-210 and polonium-210 in the atmosphere. *Tellus* 18, 427–433.
- Schötzig, U., Schrader, H., 1993. Halbwertszeiten und Photonen-Emissionswahrscheinlichkeiten von häufig verwendeten Radionukliden. In: Report PTB-Ra 16/4. Physikalisch-Technische Bundesanstalt, Braunschweig.
- Skjerdal, H., Heldal, H.E., Gäfvert, T., Gwynn, J., Strålberg, E., Sværen, I., Liebig, P.L., Kolstad, A.K., Møller, B., Komperød, M., Lind, B., Rudjord, A.L., 2015. Radioactivity in the marine environment 2011. Results from the Norwegian National Monitoring Programme (RAME). StrålevernRapport 2015. Norwegian Radiation Protection Authority, Østerås, p. 3.
- Skjerdal, H., Heldal, H.E., Gwynn, J., Strålberg, E., Møller, B., Liebig, P.L., Sværen, I., Rand, A., Gäfvert, T., Haanes, H., 2017. Radioactivity in the marine environment 2012, 2013 and 2014. Results from the Norwegian National Monitoring Programme (RAME). StrålevernRapport 2017. Norwegian Radiation Protection Authority, Østerås, p. 13.
- Skjerdal, H., Heldal, H.E., Rand, A., Gwynn, J., Jensen, L.K., Volynkin, A., Haanes, H., Møller, B., Liebig, P.L., Gäfvert, T., 2020. Radioactivity in the Marine Environment 2015, 2016 and 2017. Results from the Norwegian Marine Monitoring Programme (RAME). DSA Report 2020. Norwegian Radiation and Nuclear Safety Authority, Østerås, p. 04.
- Sternal, B., Junttila, J., Skirbekk, K., Forwick, M., Carroll, J., Pedersen, K.B., 2017. The impact of submarine copper mine tailing disposal from the 1970s on Repparfjorden, northern Norway. *Mar. Pollut. Bull.* 120, 136–153.
- Sværen, I., 2010. Caesium-137 in Sediments From Two Norwegian Fjords – Including Dating Sediment Cores. Master of Science Thesis in. Environmental Chemistry. Department of Chemistry, University of Bergen, Norway.
- Turekian, K.K., Nozaki, Y., Benninger, L.K., 1977. Geochemistry of atmospheric radon and radon products. *Annu Rev Earth Pl Sc* 5, 227–255.
- Zaborska, A., Carroll, J., Papucci, C., Torricelli, L., Carroll, M.L., Walkusz-Miotk, J., Pempkowiak, J., 2008. Recent sediment accumulation rates for the Western margin of the Barents Sea. *Deep Sea Res., Part II* 55, 2352–2360.